Zeitschrift: Schweizerische mineralogische und petrographische Mitteilungen = Bulletin suisse de minéralogie et pétrographie

Band: 83 (2003)

Heft: 2

Artikel: Primary and secondary pseudobrookite minerals in volcanic rocks from the Katzenbuckel Alkaline Complex, southwestern Germany

Autor: Stähle, Volker / Koch, Mario

DOI: https://doi.org/10.5169/seals-63141

Schweizerische Mineralogische und Petrographische Mitteilungen 83, 145–158, 2003

Primary and secondary pseudobrookite minerals in volcanic rocks from the Katzenbuckel Alkaline Complex, southwestern Germany

Volker Stähle[1] and *Mario Koch*[1]

Abstract

The Katzenbuckel volcano contains both primary and secondary pseudobrookite. Although texturally distinguishable, these Fe–Ti oxides are similar in chemical composition, albeit with some characteristic differences.
Early magmatic pseudobrookite occurs in tinguaite. In the course of crystallization pseudobrookite became unstable in the alkaline dike and in contact with titanohematite reacted to (a) ilmenite, and with the residual liquid to (b) fine-grained symplectites consisting of hematite+freudenbergite or hematite + ilmenite + magnetite + freudenbergite. Very low MgO (3.10–3.87 wt%) and relatively high FeO contents (5.66–7.38 wt%) characterize primary pseudobrookite.
Secondary, predominantly pseudomorphic pseudobrookite minerals are much more frequent and are present in various Katzenbuckel rocks. A syenite dike has niobium-rich pseudobrookite minerals with up to 8.56 wt% Nb_2O_5. Reddish, highly oxidized sanidine nephelinites contain pseudobrookite with high concentrations of 47.64 wt% Fe_2O_3 and minor contents of 4.98 wt% MgO, 0.46 wt% MnO, 0.85 wt% Al_2O_3, 0.25 wt% ZrO_2 and 0.27 wt% V_2O_5 on average.

Keywords: Pseudobrookite, tinguaite, syenite, sanidine nephelinite, Katzenbuckel volcano.

1. Introduction

Fe–Ti oxides are common accessory minerals in igneous rocks, forming solid solution series of spinel, ilmenite-hematite and pseudobrookite. Among these pseudobrookite is the most titanium-rich phase containing variable amounts of di- and trivalent iron. The pseudobrookite solid solution end-members are pseudobrookite (Fe_2TiO_5) and ferropseudobrookite ($FeTi_2O_5$), whereas isostructural armalcolite ($Fe_{0.5}Mg_{0.5}Ti_2O_5$) is restricted to members containing divalent iron. These oxides are not composed solely of iron, titanium and magnesium, but contain minor amounts of many other elements, such as Cr, Al, V, Mn, Ca, Zr, etc. (Bowles, 1988). However, in Bowles' classification the proposed definition between armalcolite and pseudobrookite is arbitrary, particularly in specimens next to the $FeTi_2O_5$ end-member composition.

Pseudobrookite occurs frequently in subaerially extruded basalts as a secondary oxidation product of ilmenite and titanomagnetite and may also be present as an exhalative new formation in vugs or miarolitic cavities of volcanic rocks (Kleck, 1970; Haggerty, 1976b; Lufkin, 1976; Parodi et al., 1989; Stormer and Zhu, 1994). Armalcolite is a typical component of lunar basalts and also has been found on Earth in some igneous rocks under highly reducing conditions (El Goresy and Chao, 1976; Haggerty, 1987; Frost and Lindsley, 1991; Hayob and Essene, 1995). Likewise, primary pseudobrookite is relatively rare in terrestrial rocks because higher cooling rates alone may prevent the reaction of pseudobrookite with the liquid to form ilmenite (Haggerty, 1976b; Wagner and Velde, 1986). Natural examples are found in some TiO_2-rich basaltic rocks (von Knorring and Cox, 1961; Rice et al., 1971; Anderson and Wright, 1972; van Kooten, 1980), in alkali gabbro (Johnston and Stout, 1984), lamprophyric minette (Wagner and Velde, 1985), and in some types of Spanish lamproites (Wagner and Velde, 1986; Venturelli et al., 1991; Brigatti et al., 1993).

The Katzenbuckel alkaline complex in SW Germany is a classic locality where pseudobrookite occurs (Fig. 1). Already ten years after the discovery of pseudobrookite by Koch (1878) in andesitic rocks of the Aranyer Berg, Lattermann (1888) found this mineral in a special type of

[1] University of Heidelberg, Mineralogisches Institut, Im Neuenheimer Feld 236, D-69120 Heidelberg, Germany. <vstaehle@min.uni-heidelberg.de>

0036-7699/03/0083/145

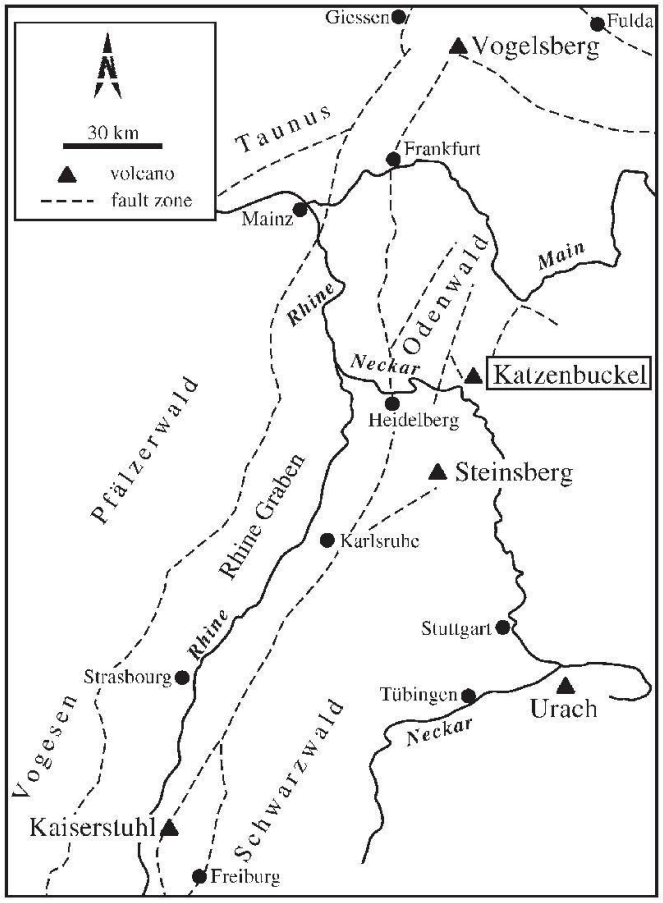

Fig. 1 Sketch map from the Rhine graben area (E-France/SW-Germany) indicating the location of the Katzenbuckel complex, ~30 km east of Heidelberg. Modified after Calvez and Lippolt (1980).

Katzenbuckel rock. Red-colored, highly oxidized sanidine nephelinites or sodium shonkinites host pseudomorphs of pseudobrookite after titanomagnetite and ilmenite (Frenzel, 1953, 1954). These highly oxidized rocks also contain hematite and a sulphur-yellow colored variety of ferridiopside (Lattermann, 1888; Frenzel, 1985). In less oxidized rocks microphyric titanomagnetite with exsolved ilmenite lamellae parallel to {111} is frequently transformed to pseudobrookite. According to Frenzel (1955, 1956) this secondary formation of pseudobrookite is due to the influence of hot volcanic gases of about 1000 °C having roasted and oxidized near surficial parts of solidifying and cooling volcanic rocks.

First analyses of pseudobrookite from the Katzenbuckel volcano were published by Lattermann (1888). Two wet chemical analyses yielded an average of 46.79 wt% TiO_2, 48.64 wt% Fe_2O_3 and 4.53 wt% MgO. These early results are in good accordance with three electron-microprobe analyses given by Ottemann and Frenzel (1965). In addition, these authors found minor contents of manganese in pseudobrookite minerals in the range of 0.5–2.5 wt% MnO. A larger dataset of pseudobrookite analyses from oxidized Katzenbuckel rocks was performed by Traub (1975).

Table 1 Major and trace elements of a tinguaite (Kb50) and a syenite (Kb58) dike.

	Kb 50 wt%	**Kb 58** wt%
SiO_2	55.16	57.27
TiO_2	1.98	2.56
Al_2O_3	11.27	14.83
Fe_2O_3 (1)	11.07	7.60
MnO	0.19	0.23
MgO	2.66	1.51
CaO	1.34	0.80
Na_2O	6.03	3.54
K_2O	6.14	9.03
P_2O_5	0.43	0.44
SO_3	0.02	0.05
LOI (2)	2.68	0.97
Total	98.97	98.83
	ppm	ppm
Cl	30	44
F	1410	808
Ba	891	543
Ce	245	186
Co	< 5	7
Cr	10	< 5
Cs	9	11
La	431	87
Nb	239	766
Ni	12	13
Pb	24	47
Rb	143	182
Sr	2937	1298
Ta	< 5	25
Th	23	66
U	13	< 5
V	56	127
Y	31	68
Zn	152	215
Zr	2813	4142

(1) All iron as Fe_2O_3
(2) LOI: loss on ignition at 1000 °C

The microscopic reexamination of a large suite of Katzenbuckel rocks lead to the detection of primary pseudobrookite within a lately intruded alkaline dike. The discovery along with the lack of good quality microprobe data from secondary pseudobrookite minerals provided the stimulus for this study. The observations and data presented here are meant to improve and complete previous studies such as Ottemann and Frenzel (1965).

2. Analytical procedures

Mineral analyses were performed using a CAMECA SX-51 microprobe (Mineralogical Institute, University Heidelberg) equipped with five wavelength-dispersive spectrometers. Operating con-

ditions were 20 nA beam current and 15 kV accelerating voltage with a beam diameter of about 1 μm. Natural as well as synthetic silicate and oxide standards were used for calibration, and data was corrected using the PAP algorithm.

Whole rock and trace elements were analyzed by X-ray fluorescence (SIEMENS SRS 3000) using melted and pressed whole rock powder tablets prepared in an agate mortar (Laboratory of Terrachem, Mannheim, Germany).

3. Mineralogy and chemical composition

3.1. Magmatic pseudobrookite

3.1.1. Primary pseudobrookite in a tinguaite dike

Pseudobrookite as a magmatic or primary crystallization product was found in a greenish-colored tinguaite rock from the Katzenbuckel. The bulk chemical and trace element composition of this clinoproxene-rich dike is shown in Table 1. High alkaline (up to 13 wt% Na_2O+K_2O) and low calcium contents (≈1 wt% CaO) are typical features of Katzenbuckel dike rocks (Stähle et al., 2002).

Alkali syenite and tinquaite dikes occur in both main country rocks of sanidine nephelinite and sodium shonkinite composition (Frenzel, 1975). A detailed mineral and chemical description of various Katzenbuckel rocks has been undertaken recently by Mann (2003).

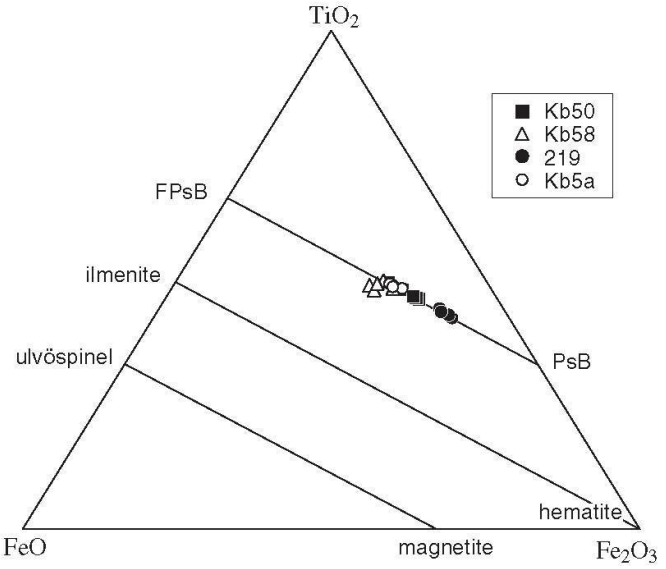

Fig. 2 Ternary composition diagram in the system TiO_2–FeO–Fe_2O_3 showing chemical composition of pseudobrookite minerals plotted as 9 cations per formula unit. Minor contents of the pseudobrookite analyses such as Nb, V and Zr were included in the Ti end-member of this system, Mg and Mn in the Fe^{2+}, and Al in the Fe^{3+} end-member.

The medium-grained, approximately 10 cm thick tinquaite dike (Kb50) intruded a sanidine nephelinite host rock. Acicular to spiky grains of Zr-rich aegirine, pleochroic, leather-brown to yellow-green katophoritic amphibole prisms and Carlsbad-twinned sanidine laths ($Or_{59.4}$ $Ab_{40.6}$) up to 3 mm in size are the main mineral constituents. Along contacts to the country rocks the dike minerals are arranged at right angle, showing comb textures, whereas in the inner parts of the dike an irregular or directionless arrangement of the rock-forming minerals is present. Many interstices are filled with dark-brown, fine-grained, nearly isotropic masses marking sites of decomposed feldspathoid minerals, possibly of nepheline. In some of these interstices natrolite is present possibly as a late magmatic crystallization product. The opaque minerals are magnetite, titanohematite, ilmenite, pseudobrookite and freudenbergite (Stähle et al., 2002). The heterogeneity of this dike, with variable grain size and uneven mineral distribution, allows only a tentative estimation of the modal composition (in volume percent): fsp 40%, foid 15%, cpx 35% and amp 10%. Each of the opaques are accessory constituents of less than 1%.

Euhedral to subhedral pseudobrookite grains are concentrated and linearly arranged about 1 cm from and parallel to the border of the dike. They show a maximum grain size of up to 1.1 mm. In transmitted light pseudobrookite is either dark red or opaque. Some grains show cleavage planes parallel to (010) or are irregularly fractured. Their chemical composition is given in Table 2. Analyses with a predominance of Fe^{3+} lie close to the end-member Fe_2TiO_5 within the ternary diagram TiO_2–FeO–Fe_2O_3 (Fig. 2).

All primary pseudobrookite grains in the tinguaite show reaction or breakdown features at grain boundaries. This indicates the onset of minerals' instability in the course of rock solidification. Decomposition experiments show that pseudobrookite breaks down at 585 ± 10 °C and intermediate members break down between 700 ° and 800 °C (Haggerty and Lindsley, 1970).

Two different processes were inferred microscopically:

1. Co-precipitated titanohematite-ilmenite pairs replace pseudobrookite at the site where grain boundaries touch. Some smaller, residual pseudobrookite grains are completely surrounded by assemblages of titanohematite-ilmenite. In all cases a smaller ilmenite seam is developed in-between residual pseudobrookite and adjacent titanohematite. From these arrangements it is deduced that ilmenite in part replaces pseudobrookite. An ilmenite-hematite mantle around a round-

Table 2 Representative electron-microprobe analyses of pseudobrookite, hematite and ilmenite of tinguaite dike Kb50. Atomic ratios of pseudobrookite were calculated on the basis of 6 cations and 10 oxygens, and for hematite and ilmenite on the basis of 2 cations and 3 oxygens.

sample	Psb Kb50-01	Psb Kb50-02	Psb Kb50-03	Psb Kb50-06	Psb Kb50-29	average	Hem Kb50-08	Hem Kb50-14	Ilm Kb50-07	Ilm Kb50-13
SiO_2	0.00	0.00	0.00	0.01	0.00	0.00	0.00	0.00	0.00	0.02
TiO_2	47.24	47.67	49.35	50.76	47.98	48.60	25.40	24.50	38.41	40.07
ZrO_2	0.12	0.17	0.15	0.27	0.10	0.16	0.04	0.05	0.04	0.03
Nb_2O_5	0.36	0.41	0.39	0.47	0.37	0.40	0.09	0.16	0.09	0.40
V_2O_5	0.17	0.19	0.23	0.24	0.30	0.23	0.16	0.18	0.10	0.17
Al_2O_3	0.00	0.00	0.00	0.00	0.00	0.00	0.00	0.00	0.00	0.00
Cr_2O_3	0.00	0.00	0.00	0.02	0.00	0.00	0.00	0.00	0.03	0.00
Fe_2O_3	42.88	42.46	39.18	36.10	41.37	40.40	54.85	56.04	29.34	25.95
FeO	5.66	5.72	6.93	7.38	6.11	6.36	18.33	18.27	25.24	27.47
MnO	0.63	0.58	0.49	0.66	0.62	0.59	1.19	1.19	2.99	4.02
MgO	3.10	3.28	3.54	3.87	3.22	3.40	1.79	1.41	3.37	2.57
CaO	0.00	0.01	0.00	0.00	0.00	0.00	0.00	0.01	0.00	0.00
Na_2O	0.01	0.01	0.00	0.02	0.04	0.02	0.06	0.06	0.07	0.09
K_2O	0.01	0.01	0.00	0.06	0.00	0.02	0.01	0.01	0.03	0.01
Total	100.17	100.52	100.27	99.84	100.11	100.18	101.91	101.87	99.70	100.79
Si	0.000	0.000	0.000	0.001	0.000		0.000	0.000	0.000	0.000
Ti	2.734	2.747	2.842	2.924	2.777		0.480	0.465	0.723	0.751
Zr	0.004	0.006	0.006	0.010	0.004		0.000	0.001	0.000	0.000
Nb	0.012	0.014	0.013	0.016	0.013		0.001	0.002	0.001	0.005
V	0.002	0.002	0.002	0.002	0.003		0.001	0.001	0.000	0.001
Al	0.000	0.000	0.000	0.000	0.000		0.000	0.000	0.000	0.000
Cr	0.000	0.000	0.000	0.001	0.000		0.000	0.000	0.001	0.000
Fe^{3+}	2.483	2.448	2.257	2.081	2.396		1.037	1.064	0.553	0.486
Fe^{2+}	0.364	0.366	0.444	0.472	0.393		0.385	0.386	0.528	0.572
Mn	0.041	0.038	0.032	0.043	0.040		0.025	0.025	0.063	0.085
Mg	0.356	0.375	0.404	0.441	0.369		0.067	0.053	0.126	0.096
Ca	0.000	0.001	0.000	0.000	0.000		0.000	0.000	0.000	0.000
Na	0.002	0.002	0.000	0.002	0.005		0.003	0.003	0.003	0.004
K	0.001	0.001	0.000	0.006	0.000		0.000	0.000	0.001	0.000
cations	6.000	6.000	6.000	6.000	6.000		2.000	2.000	2.000	2.000
oxygens	10.000	10.000	10.000	10.000	10.000		3.000	3.000	3.000	3.000

ed pseudobrookite remnant is shown in Fig. 3. Such a texture is striking evidence of the existence of primary pseudobrookite in the tinguaite rock. The high-magnification BSE-image (Fig. 3) of the ilmenite-titanohematite shell shows a multitude of fine, lens-shaped exsolution lamellae in the interior. As the tinguaite cooled further the fine exsolutions appear to have developed. Ilmenite in the mantle has higher Fe_2O_3 contents, and titanohematite is rich in titanium (Deer et al., 1992; Table 2). From the broadness of the miscibility gap of ilmenite-titanohematite pairs in the system $FeTiO_3$–Fe_2O_3 (Lindsley, 1973), crystallization temperatures in the range of 750 to 550 °C have been tentatively estimated for some alkaline dikes of the Katzenbuckel (Stähle et al., 2002).

2. A second type of reaction or decomposition process of the primary pseudobrookite is seen in small patches of symplectites at the edges of some grains. The symplectites show spotted, graphic and locally myrmekitic intergrowths of small, anhedral grains of titanohematite and freudenbergite or titanohematite, ilmenite, magnetite and freudenbergite (Fig. 4). Where such breakdown features occur, ilmenite-titanohematite reaction rims are lacking. Moreover, pseudobrookite only breaks down in places where late-stage foid minerals have precipitated. Here, the cooling residual liquid is thought to have had unhindered access and thus reacted with early crystallized pseudobrookite. Where pseudobrookite is in contact with sanidine, the original grain is unaltered.

Small anhedral magnetite grains in the breakdown assemblage can be identified in the microscope due to their white-blue maghemite coatings. These symplectitic magnetite grains are out of equilibrium with early crystallized pseudobrookite minerals. Phase relations in the FeO–TiO_2–Fe_2O_3 system show that the pair pseudobrookite + magnetite is unstable at temperatures of formation (Lindsley, 1976; Haggerty, 1976a).

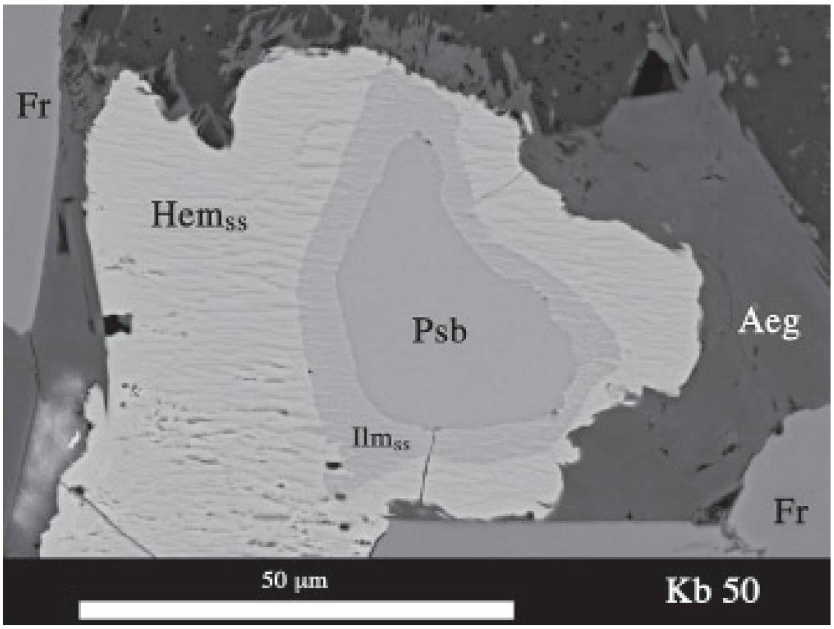

Fig. 3 BSE-image of pseudobrookite (Psb) in contact with ilmenite (Ilm) and titanohematite (Hem) within a tinguaite dike Kb50. The residual pseudobrookite grain is replaced by ilmente/hematite. Note the fine exsolution lamellae of hem$_{ss}$ in ilmenite and of ilm$_{ss}$ in titanohematite. The oxide minerals are surrounded by aegirine (Aeg) and freudenbergite (Fr).

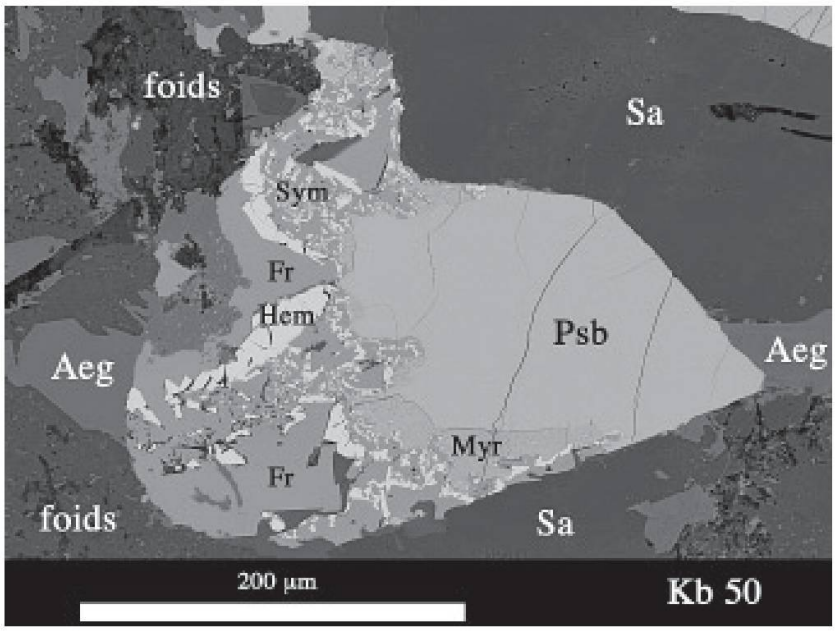

Fig. 4 BSE-image of a primary, euhedral pseudobrookite grain in tinguaite dike Kb50. On the left side pseudobrookite is replaced by symplectitic minerals (Sym), hematite (Hem) and freudenbergite (Fr). Part of the symplectites show myrmekitic intergrowths (Myr). The surrounding minerals consist of sanidine (Sa), aegirine (Aeg) and foid minerals (Foids). Note the existence of symplectite minerals predominantly at places where late-stage foid minerals occur.

Some larger, euhedral to subhedral magnetite grains occur together with freudenbergite crystals in close neighborhood. They are stable phases at some distance to early-crystallized pseudobrookite due to larger chemical inhomogeneities within the dike. Furthermore, a primary nature of pseudobrookite in this dike is also sustained due to the lack of secondary pseudobrookite in the adjacent sanidine nephelinite country rock.

3.2. Secondary pseudobrookite

3.2.1. Single crystalline and pseudomorphic niobian pseudobrookite in a syenite dike

Within a large suite of Katzenbuckel dikes one syenite vein (Kb58) contains unusually high amounts of pseudobrookite. The bulk chemical and trace element composition of the syenite is listed in Table 1. The syenite is richer in potassium

Table 3 Representative electron-microprobe analyses of pseudobrookite minerals from syenite dike Kb58. The chemical range of 48 pseudobrookite analyses from the same dike is also shown. The atomic ratios of pseudobrookite were calculated on the basis of 6 cations and 10 oxygens.

sample	Psb Kb58-05	Psb Kb58-78	Psb Kb58-13	Psb Kb58-40	Psb Kb58-32	range of 48 analyses Min	Max
SiO_2	0.00	0.00	0.00	0.00	0.02	0.00	0.03
TiO_2	45.99	47.16	44.29	48.39	51.63	43.11	51.81
ZrO_2	0.33	0.67	0.38	0.51	0.12	0.10	0.96
Nb_2O_5	6.68	3.97	7.51	1.74	0.73	0.09	8.56
V_2O_5	0.33	0.61	0.41	0.34	0.32	0.21	0.61
Al_2O_3	0.00	0.00	0.00	0.00	0.13	0.00	0.19
Cr_2O_3	0.00	0.03	0.01	0.04	0.03	0.00	0.06
Fe_2O_3	32.93	33.55	34.09	37.37	35.19	31.55	38.61
FeO	6.63	6.70	6.62	5.34	6.36	4.79	7.51
MnO	1.32	1.14	1.13	0.96	0.60	0.59	1.40
MgO	5.52	4.81	5.47	4.73	4.94	4.22	5.61
CaO	0.00	0.00	0.00	0.00	0.03	0.00	0.07
Na_2O	0.04	0.02	0.00	0.00	0.00	0.00	0.04
K_2O	0.00	0.06	0.00	0.00	0.02	0.00	0.06
Total	99.76	98.71	99.91	99.42	100.11	98.11	101.88
Si	0.000	0.000	0.000	0.000	0.001	0.000	0.002
Ti	2.676	2.772	2.587	2.801	2.943	2.558	2.960
Zr	0.012	0.025	0.014	0.019	0.005	0.004	0.036
Nb	0.234	0.140	0.264	0.061	0.025	0.003	0.305
V	0.003	0.006	0.004	0.003	0.003	0.002	0.006
Al	0.000	0.000	0.000	0.000	0.011	0.000	0.017
Cr	0.000	0.002	0.000	0.002	0.002	0.000	0.003
Fe^{3+}	1.917	1.973	1.992	2.165	2.006	1.850	2.256
Fe^{2+}	0.429	0.438	0.430	0.343	0.403	0.300	0.484
Mn	0.086	0.076	0.074	0.063	0.039	0.037	0.093
Mg	0.636	0.560	0.633	0.542	0.558	0.488	0.653
Ca	0.000	0.000	0.000	0.000	0.002	0.000	0.006
Na	0.005	0.002	0.000	0.000	0.000	0.000	0.006
K	0.000	0.006	0.000	0.000	0.002	0.000	0.006
cations	6.000	6.000	6.000	6.000	6.000	6.000	6.000
oxygens	10.000	10.000	10.000	10.000	10.000	10.000	10.000

and has higher niobium and zirconium contents than the tinguaite dike described above.

The thin, grey- to light-brown colored dike within sanidine nephelinite has a thickness of about 1.5 cm. Macroscopically, the medium-grained dike contains tabular or blocky, mm-sized sanidine crystals and some dark-brown, katophoritic amphibole laths, up to 3 mm long. Masses of tabular sanidine crystals form the bulk texture of the dike. Thin seams of smaller grain size on both sides of the dike indicate that intrusion followed cooling of the sanidine nephelinite country rock.

In addition to Carlsbad-twinned sanidine and pleochroic amphibole, red colored biotite and greenish aegirine occur within the dike. Shown with many examples biotite overgrows amphibole. Part of the sanidine interstices are filled with zeolites. Accessories are zircon, ilmenite, titanohematite and some magnetite grains, the latter being partly transformed into maghemite. Numerous pseudobrookite crystals are present as a minor constituent of the dike. The modal composition of the syenite rock is (in volume percent): sanidine 60%, amphibole 20%, biotite 7%, aegirine 3%, zeolite 3%, pseudobrookite 5%, zircon <1% and each of the opaques ≈1%.

Pseudobrookite grains show two different types of occurrence within the syenite dike. Most grains occur as single, subhedral to anhedral or roundish crystals in the interstices of sanidine laths. Some of them touch small magnetite grains. To a lesser extent, pseudobrookite is present in xenomorphic patches, intergrown with magnetite (Fig. 5). However, magnetite-pseudobrookite grain boundaries indicate a mineral association that can not be in equilibrium at individual crystallization temperatures. Careful checking of such xenomorphic pseudobrookite grains revealed the replacement of pre-existing ilmenite. This can be seen in Fig. 5 where a small residual island of ilmenite and titanohematite is completely surrounded by pseudobrookite. From these observa-

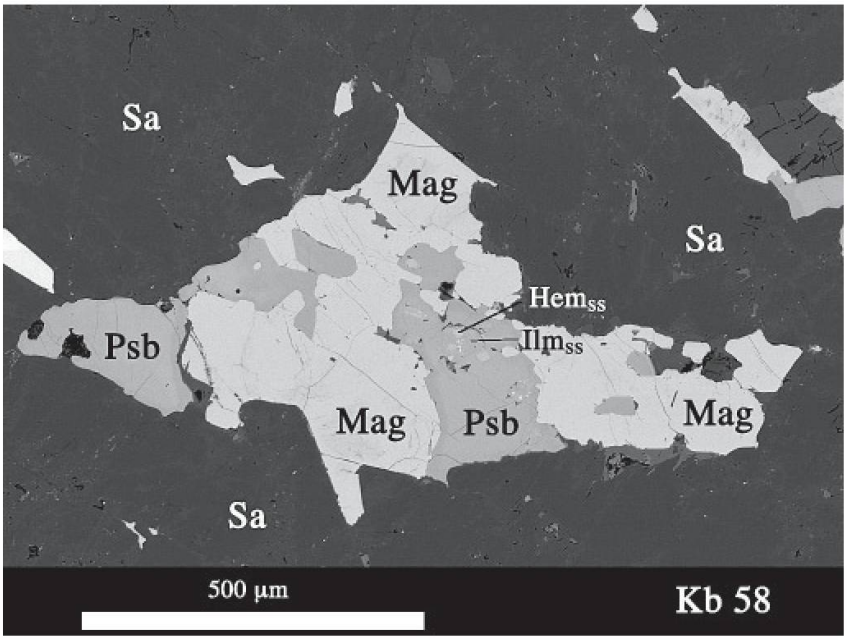

Fig. 5 BSE-image of a magnetite (Mag)–pseudobrookite (Psb) intergrowth. Secondary pseudobrookite minerals replace pre-existing ilmenite. A small island of primary hematite (Hem) and ilmenite (Ilm) can be seen in the center. The surrounding minerals are sanidine feldspars (Sa).

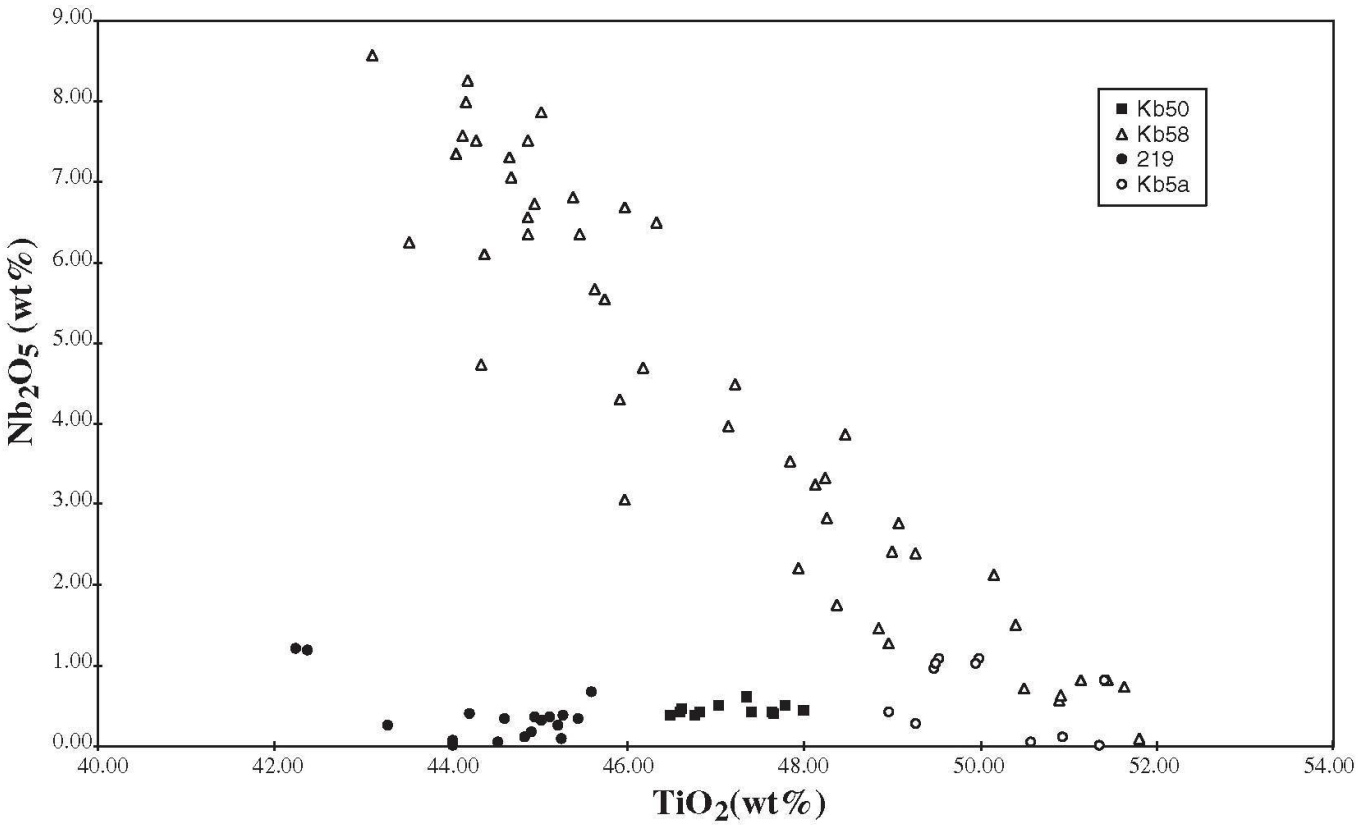

Fig. 6 Distribution of Nb_2O_5 and TiO_2 contents in pseudobrookite from different Katzenbuckel rocks. Secondary pseudobrookite minerals with anomalous high niobian contents occur in the syenite dike Kb58.

tions we conclude that all pseudobrookite in the syenite dike (Kb58) is secondary in origin. Furthermore, the sanidine nephelinite country rock also contains some secondarily formed pseudobrookite. Some of the microphyric titanomagnetite grains in the matrix of the sanidine nephelinite show pseudobrookite minerals which replace exsolved ilmenite lamellae.

The chemical composition of the pseudobrookite crystals in the syenite is shown in Fig. 2. The large variation in approximately 50 mineral analyses reveals that pseudobrookite grains are

Table 4 Representative electron-microprobe analyses of pseudobrookite, hematite and magnetite from the red-colored sanidine nephelinite rock 219. The atomic ratios of pseudobrookite were calculated on the basis of 6 cations and 10 oxygens, hematite on the basis of 2 cations and 3 oxygens, and magnetite on the basis of 3 cations and 4 oxygens.

sample	Psb in mag 219-102	Psb in mag 219-105	Psb in mag 219-116	Psb in mag 219-127	Psb in matrix 219-122	average	Hem in mag 219-101	Hem in mag 219-112	Mag host 219-100	Mag host 219-115
SiO_2	0.03	0.03	0.16	0.04	0.02	0.06	0.12	0.02	0.00	0.05
TiO_2	44.02	44.93	44.84	45.27	45.46	44.90	14.81	14.92	2.25	2.47
ZrO_2	0.09	0.28	0.04	0.33	0.53	0.25	0.00	0.00	0.00	0.00
Nb_2O_5	0.00	0.17	0.11	0.07	0.33	0.14	0.02	0.02	0.02	0.00
V_2O_5	0.26	0.18	0.43	0.28	0.19	0.27	0.13	0.09	0.07	0.00
Al_2O_3	1.58	0.15	1.83	0.27	0.40	0.84	0.87	0.75	8.49	10.31
Cr_2O_3	0.01	0.00	0.03	0.00	0.01	0.01	0.03	0.04	0.00	0.00
Fe_2O_3	48.21	47.36	47.50	48.14	46.97	47.64	75.47	75.35	63.26	60.72
FeO	0.00	0.00	0.00	0.00	0.02	0.00	1.90	2.11	5.93	5.06
MnO	0.19	0.73	0.24	0.53	0.59	0.46	0.99	1.05	4.44	4.25
MgO	4.77	5.01	4.83	5.19	5.10	4.98	5.81	5.72	15.70	16.48
CaO	0.02	0.03	0.00	0.01	0.07	0.03	0.01	0.00	0.00	0.02
Na_2O	0.03	0.02	0.09	0.00	0.04	0.03	0.05	0.02	0.02	0.06
K_2O	0.02	0.04	0.01	0.01	0.07	0.03	0.00	0.01	0.01	0.00
Total	99.24	98.91	100.09	100.13	99.80	99.64	100.21	100.11	100.21	99.42
Si	0.002	0.002	0.012	0.003	0.002		0.003	0.001	0.000	0.002
Ti	2.527	2.599	2.546	2.586	2.602		0.277	0.280	0.056	0.060
Zr	0.003	0.010	0.002	0.012	0.020		0.000	0.000	0.000	0.000
Nb	0.000	0.006	0.004	0.002	0.011		0.000	0.000	0.000	0.000
V	0.003	0.002	0.004	0.003	0.002		0.000	0.000	0.000	0.000
Al	0.142	0.013	0.163	0.024	0.036		0.025	0.022	0.328	0.395
Cr	0.001	0.000	0.001	0.000	0.000		0.001	0.001	0.000	0.000
Fe^{3+}	2.769	2.740	2.699	2.751	2.690		1.414	1.415	1.561	1.485
Fe^{2+}	0.000	0.000	0.000	0.000	0.002		0.040	0.044	0.163	0.138
Mn	0.012	0.047	0.015	0.034	0.038		0.021	0.022	0.123	0.117
Mg	0.543	0.574	0.543	0.587	0.578		0.216	0.213	0.767	0.799
Ca	0.001	0.003	0.000	0.001	0.006		0.000	0.000	0.000	0.001
Na	0.004	0.002	0.013	0.000	0.006		0.003	0.001	0.001	0.004
K	0.002	0.004	0.001	0.001	0.007		0.000	0.000	0.000	0.000
cations	6.010	6.003	6.003	6.004	6.000		2.000	2.000	3.000	3.000
oxygens	10.000	10.000	10.000	10.000	10.000		3.000	3.000	4.000	4.000

heterogeneous, particularly in niobium content (Table 3). The large scatter of Nb_2O_5, in the range of 0.09–8.56 wt%, is demonstrated in Fig. 6. Even within single grains, niobium is inhomogeneously distributed, which can also be seen in the BSE-images. Altogether, numerous electron-microprobe analyses show that both pseudobrookite varieties in this sample are chemically indistinguishable (Table 3).

3.2.2. Pseudobrookite pseudomorphs in oxidized sanidine nephelinite (red type)

Sodium-rich sanidine nephelinites are the main rock type of the Katzenbuckel volcano. The fine-grained, melanocratic volcanics are in part porphyric containing clinopyroxene phenocrysts. Main mineral constituents are sanidine, nepheline, nosean, diopsidic pyroxene, olivine, biotite, hornblende and apatite. The opaques are present as titanomagnetite and ilmenite minerals with modes of up to 15 vol% (Frenzel, 1975). Euhedral titanomagnetite grains are either microphyric or occur as tiny crystals within the matrix.

The red-colored, pseudobrookite-rich rock was found as a 30 cm-sized sanidine nephelinite boulder (sample 219) in the northwest corner of the Michelsberg quarry.

All Fe–Ti oxides of the groundmass are completely transformed into pseudobrookite or hematite, giving this type of volcanic rock its conspicuous reddish color. Similar, highly oxidized, martite- and pseudobrookite-bearing rocks were described by Frenzel (1953, 1975).

The highly oxidized rock typically contains ferridiopsides of wine-yellow or sulfur-yellow colors (Frenzel, 1985). Olivine is completely decomposed to accumulations of tiny hematite

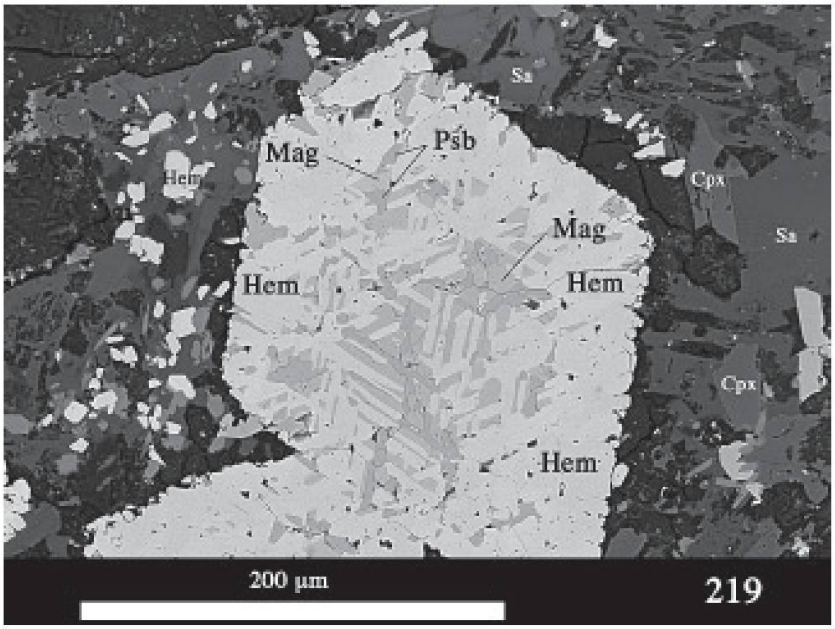

Fig. 7 BSE-image of a microphyric titanomagnetite in the red-colored sanidine nephelinite (219) containing newly formed hematite (Hem) and pseudobrookite (Psb). Note the residual titanomagnetite (Mag) blebs in central parts of the grain. In the surrounding matrix fine-grained sanidine (Sa), clinopyroxene (Cpx) and hematite (Hem) minerals occur.

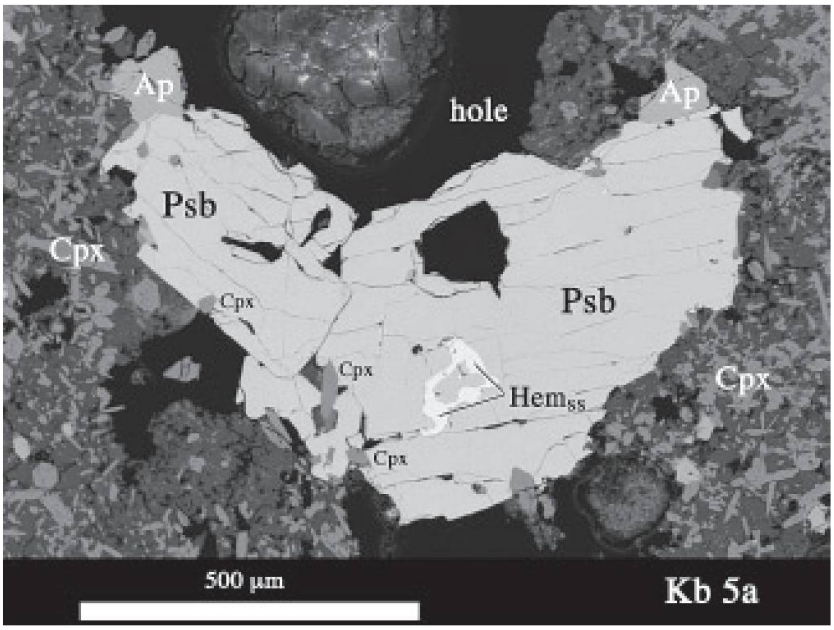

Fig. 8 BSE-image of euhedral to subhedral pseudobrookite (Psb) crystals in a volcanic cavity or hole of the sanidine nephelinite Kb5a. The ring-shaped inclusion in one of the pseudobrookite grains is hematite (Hem_{ss}). Small clinopyroxene crystals (Cpx) included in pseudobrookite are pre-existing constituents of the sanidine nephelinite matrix. Apatite (Ap) and clinopyroxene occur in the surrounding matrix.

grains. Apatite full of tiny vesicles is slightly reddish. Most of the microphyric titanomagnetite is entirely transformed to hematite-pseudobrookite assemblages. Some titanomagnetite grains show relic areas of the host in central-most regions (Fig. 7). These areas are isotropic, dark brown colored and contain large concentrations of exsolved aluminous-magnesio-ferrite (Table 4).

In transmitted light, many tiny pseudobrookite crystals in the groundmass are transparent and reddish colored, whereas numerous, newly formed hematite crystals are opaque or semi-opaque with red colors at grain boundaries.

The chemical composition of the secondary pseudobrookite minerals is shown in Fig. 2 and listed in Table 4. Also shown in Table 4 are two analyses of newly formed hematite within a pre-existing titanomagnetite crystal (Fig. 7). The hematites contain unusually high concentrations of 5.40 wt% MgO, 0.73 wt% MnO and 0.86 wt%

Table 5 Representative electron-microprobe analyses of pseudobrookite, hematite and magnetite from the grey-colored sanidine nephelinite rock Kb5a. Atomic ratios for pseudobrookite were calculated on the basis of 6 cations and 10 oxygens, for hematite on the basis of 2 cations and 3 oxygens, and for magnetite on the basis of 3 cations and 4 oxygens.

	Psb	Psb	Psb	Psb	Psb	average	Hem	Hem	Mag	Mag
	big x	big x	lamella	lamella	lamella		inclusion	inclusion	x with lamella	x with lamella
	fig.8		fig.9	fig.9	fig.9		fig.8		fig.9	fig.9
sample	Kb5a-133	Kb5a-140	Kb5a-136	Kb5a-137	Kb5a-138		Kb5a-130	Kb5a-143	Kb5a-135	Kb5a-139
SiO_2	0.00	0.00	0.10	0.08	0.04	0.07	0.00	0.00	0.00	0.02
TiO_2	49.99	49.95	50.58	50.93	51.35	50.95	22.73	22.50	3.21	3.16
ZrO_2	0.17	0.18	0.13	0.12	0.10	0.12	0.00	0.00	0.00	0.00
Nb_2O_5	1.07	1.01	0.04	0.11	0.01	0.05	0.14	0.14	0.03	0.00
V_2O_5	0.29	0.24	0.29	0.30	0.35	0.31	0.20	0.23	0.14	0.18
Al_2O_3	0.00	0.00	0.58	0.62	0.54	0.58	0.00	0.00	2.15	2.12
Cr_2O_3	0.04	0.00	0.04	0.01	0.02	0.02	0.00	0.00	0.02	0.03
Fe_2O_3	37.21	37.50	38.58	36.66	36.01	37.08	59.40	58.75	62.99	62.43
FeO	4.86	4.80	2.15	3.12	3.22	2.83	14.38	15.29	23.85	23.34
MnO	0.69	0.70	0.35	0.50	0.50	0.45	1.33	1.24	2.71	2.85
MgO	5.18	5.19	6.24	6.19	6.26	6.23	2.64	2.10	5.08	4.94
CaO	0.00	0.02	0.01	0.00	0.02	0.01	0.02	0.01	0.00	0.01
Na_2O	0.04	0.01	0.06	0.00	0.00	0.02	0.04	0.03	0.02	0.04
K_2O	0.00	0.00	0.05	0.00	0.01	0.02	0.00	0.01	0.00	0.03
Total	99.52	99.59	99.21	98.62	98.41	98.75	100.87	100.30	100.19	99.15
Si	0.000	0.000	0.008	0.006	0.003		0.000	0.000	0.000	0.001
Ti	2.868	2.863	2.867	2.905	2.934		0.432	0.432	0.088	0.088
Zr	0.006	0.007	0.005	0.004	0.004		0.000	0.000	0.000	0.000
Nb	0.037	0.035	0.001	0.004	0.000		0.002	0.002	0.000	0.000
V	0.003	0.002	0.003	0.003	0.004		0.001	0.001	0.001	0.001
Al	0.000	0.000	0.052	0.055	0.049		0.000	0.000	0.093	0.092
Cr	0.002	0.000	0.002	0.000	0.001		0.000	0.000	0.001	0.001
Fe^{3+}	2.136	2.150	2.188	2.093	2.059		1.131	1.130	1.729	1.732
Fe^{2+}	0.310	0.306	0.136	0.198	0.204		0.304	0.327	0.727	0.720
Mn	0.045	0.045	0.023	0.032	0.032		0.028	0.027	0.084	0.089
Mg	0.588	0.590	0.701	0.699	0.709		0.100	0.080	0.276	0.272
Ca	0.000	0.001	0.001	0.000	0.002		0.001	0.000	0.000	0.001
Na	0.005	0.001	0.009	0.000	0.000		0.002	0.000	0.001	0.003
K	0.000	0.000	0.005	0.000	0.001		0.000	0.000	0.000	0.001
cations	6.000	6.000	6.000	6.000	6.000		2.000	2.000	3.000	3.000
oxygens	10.000	10.000	10.000	10.000	10.000		3.000	3.000	4.000	4.000

Al_2O_3 on average. The highly oxidized nature of the red-colored sanidine nephelinite rock is also reflected in the composition of pseudobrookite having almost all iron in the trivalent state.

3.2.3. Single crystalline and pseudomorphic pseudobrookite in less oxidized sanidine nephelinite (grey type)

Grey-colored sanidine nephelinites containing newly formed hematite and different types of pseudobrookite minerals (see Frenzel, 1953) were sampled at the northern wall rocks of the Michelsberg quarry. There, sanidine nephelinite rocks are in contact with the "schlot breccia" reflecting high-temperature alkali metasomatic phenomena (Frenzel, 1960). These volcanic rocks contain lesser amounts of secondary pseudobrookite and hematite than the red-colored variety and seem to be less oxidized.

Larger, single crystals of pseudobrookite and hematite predominantly settle in perforated areas within the volcanics. Local porosity at some places of sanidine nephelinite may be produced by leaching (Frenzel, 1953). These euhedral to subhedral pseudobrookite grains with planar faces crystallized from hot vapors. Such individual grains of newly formed pseudobrookite are up to 600 μm in diameter (Fig. 8). The crystals contain straight to bent cleavage planes and small hematite inclusions. Small clinopyroxene crystals from the sanidine nephelinite host are also incorporated along pseudobrookite margins. The chemical compositions of pseudobrookite crystals and hematite inclusions are listed in Table 5.

Microphyric titanomagnetite crystals with

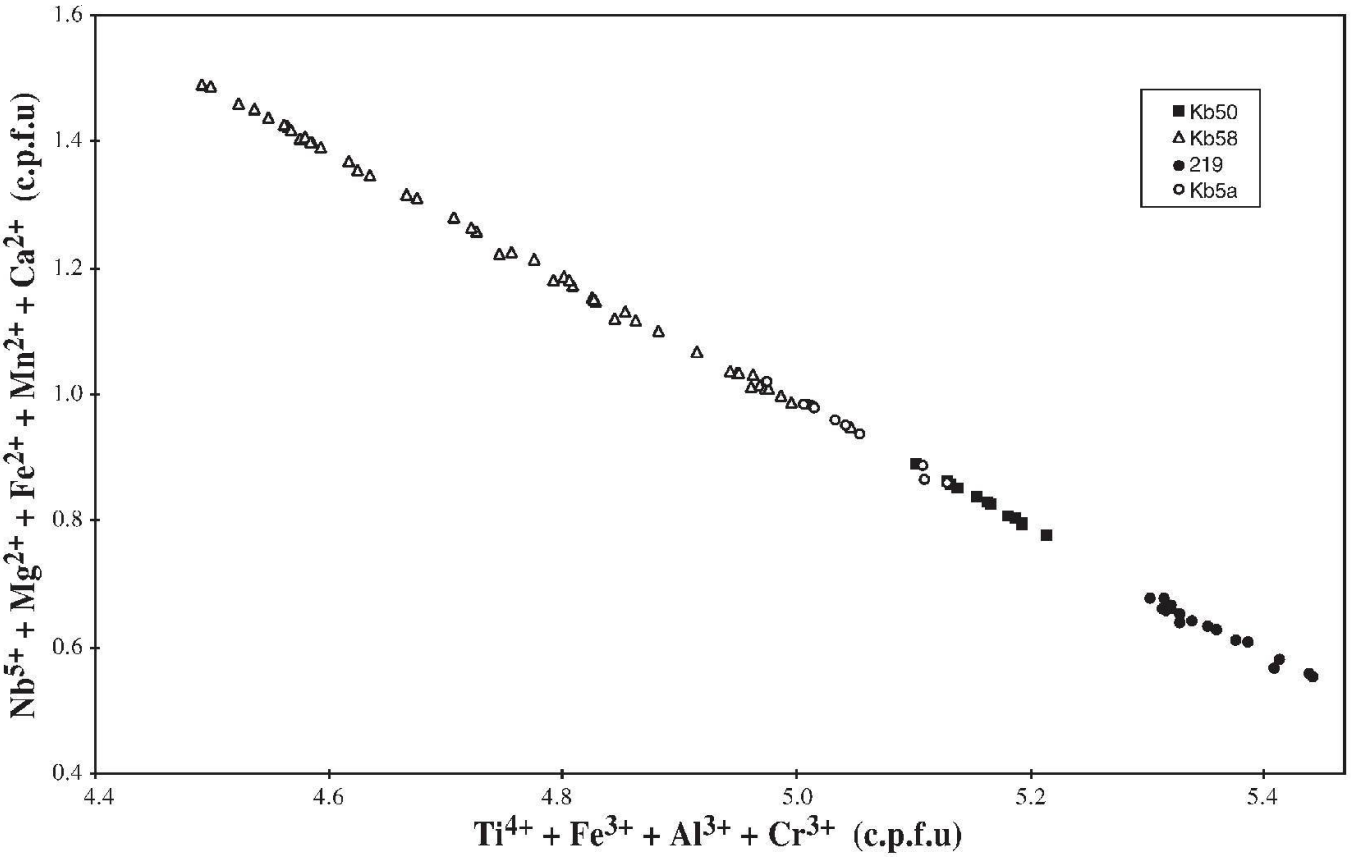

Fig. 9 Elemental plot of cations per formula unit (c.p.f.u.) shows a good correlation of the coupled substitution $Nb^{5+} + (Mg^{2+},Fe^{2+},Mn^{2+}) \leftrightarrow Ti^{4+} + Fe^{3+}$.

pseudobrookite replacing exsolved ilmenite lamellae are typical features of oxidized Katzenbuckel rocks (Fig. 2 in Frenzel, 1956). The lamellar pseudobrookite pseudomorphs contain some smaller blebs of titanohematite that are likely the result of an incomplete reaction (Haggerty, 1976a). The chemical composition of such pseudobrookite pseudomorphs and titanomagnetite host are also listed in Table 5.

4. Discussion and conclusions

The Katzenbuckel volcano is a classic locality where various types of pseudobrookite minerals occur. Both primary and secondary pseudobrookite occur and representative electron-microprobe analyses document their spread in chemical composition (Tables 2, 3, 4 and 5).

1. Primary, magmatic pseudobrookite has only been found in a tinguaite rock. Tinguaite and alkali syenite dikes are late-magmatic, highly differentiated rocks. Compared to the chemical composition of sanidine nephelinites (Frenzel, 1975), they are richer in SiO_2 and K_2O but have much lower contents of MgO, CaO and P_2O_5. In their trace element contents they are visibly enriched in niobium and zirconium.

Primary pseudobrookite has the lowest MgO content and its calculated Fe^{2+}/Fe^{3+} ratios are higher than those of secondary pseudobrookite grown within the red-colored sanidine nephelinite. Obviously, the latter minerals crystallized under highly oxidized conditions, as reflected by their high Fe^{3+} contents (Table 4).

Pseudobrookite in the tinguaite shows minor elemental concentrations of 3.40 wt% MgO and 0.59 wt% MnO. Moreover, this early-crystallized Fe–Ti oxide has on average minor contents of 0.40 wt% Nb_2O_5, 0.16 wt% ZrO_2 and zero Al_2O_3. Vanadium oxide is present in the analyses with minor concentrations of 0.23 wt% on average (Table 2). Comparable in ionic size, vanadium (V^{5+}) replaces titanium (Ti^{4+}) in the pseudobrookite structure.

Experimentally, pseudobrookite is unstable below 600 °C (Haggerty and Lindsley, 1970). Primary pseudobrookite in the tinguaite sample Kb50 shows two decomposition processes. In contact with titanohematite, ilmenite mantles and replaces pseudobrookite. Haggerty (1976b) reports a similar mechanism, namely that in the absence of rapid chilling, pseudobrookite reacts with the residual liquid to form Mg-rich ilmenite. With access of residual melt to the magmatic precipitates a second type of decomposition reaction was found in tinguaite Kb50. Fine-grained symplec-

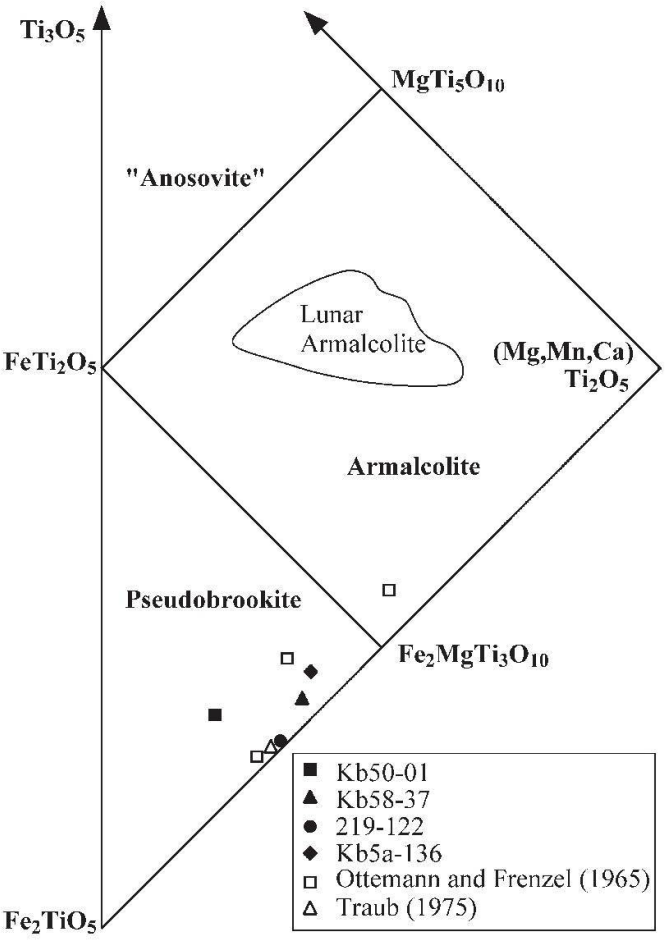

Fig. 10 Representative pseudobrookite analyses from various Katzenbuckel rocks plotted in a diagram with end-members calculated according to Bowles (1988). Three pseudobrookite analyses from Ottemann and Frenzel (1965) and the average of pseudobrookite analyses from Traub (1975) are also shown. All pseudobrookite analyses lie close together in a narrow field within the pseudobrookite triangle except one Mg-rich analysis from the latter authors. Primary pseudobrookite (Kb50-01) with the lowest MgO content (see Tables 2 to 5) plots closest to the tie-line Fe_2TiO_5–$FeTi_2O_5$.

tites at the edges of some pseudobrookite grains are composed of variable hematite, ilmenite, magnetite and freudenbergite assemblages.

2. Late-magmatic pseudobrookite is present in a variety of volcanic rocks. Syenite dike Kb58 with a lot of secondary pseudobrookite is rich in zirconium and niobium. The felsic syenite contains accessory zircon crystals up to 400 μm in size, and niobium enters preferentially into Ti-rich minerals. Compared to the tinguaite dike, the syenite has less iron but more titanium. However, the high titanium content of syenite Kb58 is likely caused in part by secondary mass supply either as vapor or liquid. Possible evidence for this is the occurrence of a large amount of single pseudobrookite crystals that grew frequently in the interstices of sanidine crystals. Likewise, this rock expresses a distinct disequilibrium due to the presence of primary ilmenite grains together with pseudobrookite pseudomorphs after ilmenite touching magnetite.

Secondary pseudobrookite in the syenite is niobium-rich, with up to 8.56 wt% Nb_2O_5. In a Slovakian granitic pegmatite, high contents of Nb (6.06 to 10.11 wt% Nb_2O_5) and Ta (0.46 to 5.15 wt% Ta_2O_5) were found in armalcolite-pseudobrookite exsolutions within rutile hosts (Uher et al., 1998). Their analyses commonly yielded a stoichiometry close to $A^{2+}B^{4+,5+}{}_2O_5$, the same as the Katzenbuckel analyses. Nb-rich pseudobrookite shows somewhat higher Mg^{2+} contents, but lower Ti^{4+} and Fe^{3+} contents compared to pseudobrookite with low Nb concentrations. This suggests the coupled substitution of $Fe^{3+} + Ti^{4+} \leftrightarrow Mg^{2+} + Nb^{5+}$ and such a good solid-solution behaviour is graphically shown in Fig. 9.

The high niobium content of the pseudobrookite likely comes from the niobium-rich syenite dike itself. In general Katzenbuckel alkali syenite dikes are rich in niobium (Stähle et al., 2002) and secondary pseudobrookite minerals in the adjacent sanidine nephelinite country rock have low concentrations of niobium. Thus, the niobium-rich pseudobrookite in syenite Kb58 is possibly a deuteric product which was developed not until the emplacement of the dike.

3. Chemically, primary pseudobrookite minerals are not very different from secondary ones. This is shown in the compositional diagrams in Figs. 2 and 10, where the pseudobrookite analyses overlap or lie close together. Likewise, the four representative pseudobrookite analyses of this study in Fig. 10 are similar to two electron-microprobe analyses of Ottemann and Frenzel (1965), whereas one of their pseudobrookite analyses lies within the "armalcolite" field. This is rather unusual and could not be confirmed. Further analyses of secondary pseudobrookite minerals from other volcanics (analyses no. 14–20 in Ottemann and Frenzel, 1965) would lie in the same "pseudobrookite" area within the diagram of Fig. 10.

The chemical difference in the diagrams are largest between primary pseudobrookite (Kb50) and secondary pseudobrookite (219). This mainly results from the higher oxidation state of the secondary pseudobrookite in the red-colored variety of sanidine nephelinite rocks.

Frenzel (1985) explained the high-temperature oxidation of the red-colored rock variety with masses of secondary pseudobrookite minerals with a fumarolic activity within the volcano. This is supported by the finding of euhedral pseu-

dobrookite crystals in cavities of sanidine nephelinite (Kb5a) which are likely products of a late-magmatic, hot gaseous flow through parts of the Katzenbuckel volcanic rocks.

Although similar in chemical composition, primary and secondary pseudobrookite minerals are clearly distinguished by their textural appearances. Primary pseudobrookite reacts with the hot residual liquid and decomposes to fine-grained symplectites or in contact with titanohematite small ilmenite seams have developed preserving the early-magmatic precipitates. In contrast, secondary pseudobrookite lacks any reaction or breakdown features and in most cases forms pseudomorphs after other rock-forming Fe–Ti oxides. Secondary pseudobrookite occurs more frequently and is found in such parts of Katzenbuckel rocks where subsequent oxididation has taken place.

Acknowledgements

We thank R. Altherr, A. ElGoresy and C. McCammon for their critical comments and much constructive advice. G. Frenzel, who collected part of the studied samples of Katzenbuckel rocks some years ago, is also thanked for critical remarks. H.-P. Meyer kindly supported us with extensive microprobe logistics, and I. Glass and M. Kaliwoda are thanked for their help with extensive BSE-imaging and assistance with the collection of microprobe data, respectively.

References

Anderson A.T. and Wright T.L. (1972): Phenocrysts and glass inclusions and their bearing on oxidation and mixing of basaltic magmas, Kilauea Volcano, Hawaii. *Am. Mineral.* **57**, 188–216.

Bowles, J.F.W. (1988): Definition and range of composition of naturally occurring minerals with the pseudobrookite structure. *Am. Mineral.* **73**, 1377–1383.

Brigatti, M.F., Contini, S., Capredi, S. and Poppi, L. (1993): Crystal chemistry and cation ordering in pseudobrookite and armalcolite from Spanish lamproites. *Eur. J. Mineral.* **5**, 73–84.

Calvez, J.-Y. and Lippolt, H.J. (1980): Strontium isotope constraints to the Rhine graben volcanism. *Neues Jahrb. Mineral. Abh.* **139**, 59–81.

Deer, W.A., Howie, R.A. and Zussmann, J. (1992): An introduction to the rock-forming minerals. Longman, Essex, 2nd edition.

El Goresy, A. and Chao, E.C.T. (1976): Identification and significance of armalcolite in the Ries glass. *Earth Planet. Sci. Lett.* **30**, 200–208.

Frenzel, G. (1953): Die Erzparagenese des Katzenbuckels im Odenwald. *Heidelberger Beitr. Mineral. und Petrogr.* **3**, 409–444.

Frenzel, G. (1954): Erzmikroskopische Beobachtungen an natürlich erhitzten, insbesondere pseudobrookitführenden Vulkaniten. *Heidelberger Beitr. Mineral. und Petrogr.* **4**, 343–376.

Frenzel, G. (1955): Einführung in die Geologie und Petrographie des Katzenbuckels im Odenwald. *Aufschluß*, Sb. **5** (Odenwald), 48–56.

Frenzel, G. (1956): Zur Kenntnis der Eisentitanoxyde in thermometamorphen Gesteinen. *Heidelberger Beitr. Mineral. und Petrogr.* **5**, 165–170.

Frenzel, G. (1960): Die neuerschlossene Schlotbreccie am Katzenbuckel im Odenwald und ihre Randgesteine. *Neues Jahrb. Mineral.* Abh. **94**, 1333–1358.

Frenzel, G. (1975): Die Nephelingesteinsparagenese des Katzenbuckels im Odenwald. *Aufschluss*, Sb. **27** (Odenwald), 213–228.

Frenzel, G. (1985): Kristallchemische Untersuchungen an Ferridiopsiden des Katzenbuckels (Odenwald, BRD). *Chem. Erde* **44**, 299–309.

Frost, B.R. and Lindsley, D.H. (1991): Occurrence of iron-titanium oxides in igneous rocks. In: Lindsley, D.H. (ed.): Oxide minerals. *Rev. Mineral.* **25**, 433–468

Haggerty, S.E. (1976a): Oxidation of opaque mineral oxides in basalts. In: Rumble, D., III (ed.): Oxide minerals. *Mineral. Soc. Am. Short Course Notes* **3**: Hg 1–Hg 100.

Haggerty, S.E. (1976b): Opaque mineral oxides in terrestrial igneous rocks. In: Rumble, D., III (ed.): Oxide minerals. *Mineral. Soc. Am. Short Course Notes* **3**, Hg 101–Hg 300.

Haggerty, S.E. (1987): Metasomatic mineral titanates in upper mantle xenoliths. In: Nixon, P.H. (ed.): Mantle xenoliths. John Wiley and Sons, New York, 671–690.

Haggerty, S.E. and Lindsley, D.H. (1970): Stability of the pseudobrookite (Fe_2TiO_5) – ferropseudobrookite ($FeTi_2O_5$) series. *Carnegie Inst. Washington, Yearb.* **68**, 247–249.

Hayob, J.L. and Essene ,E.J. (1995): Armalcolite in crustal paragneiss xenoliths, central Mexico. *Am. Mineral.* **80**, 810–822.

Johnston, A.D. and Stout, J.H. (1984): A highly oxidized ferrian salite-, kennedyite-, forsterite-, and rhönite-bearing alkali gabbro from Kauai, Hawaii and its mantle xenoliths. *Am. Mineral.* **69**, 57–68.

Kleck, W.D. (1970): Cavity minerals at summit rock, Oregon. *Am. Mineral.* **55**, 1396–1404.

Koch, A. (1878): Neue Minerale aus dem Andesit des Aranyer Berges in Siebenbürgen. *Tschermaks Mineral. Petrogr. Mitt.*, N.F. **1**, 331–361.

Lattermannn, G. (1888): Untersuchungen über den Pseudobrookit. *Tschermaks Mineral. Petrogr. Mitt.*, N.F. **9**, 47–54.

Lindsley, D.H. (1973): Delimitation of the hematite-ilmenite miscibility gap. *Geol. Soc. Am. Bull.* **84**, 657–662.

Lindsley, D.H. (1976): Experimental studies of oxide minerals. In: Rumble, D., III (ed.): Oxide minerals. *Mineral. Soc. Am. Short Course Notes* 3, L 61–L 88.

Lufkin, J.L. (1976): Oxide minerals in miarolitic rhyolite, Black Range, New Mexico. *Am. Mineral.* **61**, 425–430.

Mann, U. (2003): Petrographie und Mineralchemie von Gesteinen des Katzenbuckels. Diploma thesis, unpublished, Universität Tübingen.

Ottemann, J. and Frenzel, G. (1965): Der Chemismus der Pseudobrookite von Vulkaniten. *Schweiz. Mineral. Petrogr. Mitt.* **45**, 819–836.

Parodi, G.C., Ventura, G.D. and Lorand, J.-P. (1989): Mineralogy and petrology of an unusual osumulite + vanadium-rich pseudobrookite assemblage in an ejectum from the Vico Volcanic Complex (Latium, Italy). *Am. Mineral.* **74**, 1278–1284.

Rice, J.M., Dickey, J.S. and Lyons, J.B. (1971): Skeletal crystallization of pseudobrookite. *Am. Mineral.* **56**, 158–162.

Stähle, V., Koch, M., McCammon, C.A., Mann, U. and Markl, G. (2002): Occurrence of low-Ti and high-Ti freudenbergite in alkali syenite dikes from the Katzenbuckel volcano, southwestern Germany. *Canad. Mineral.* **40**, 1609–1627.

Stormer, J.C. and Zhu, J. (1994): Pseudobrookite and Ti-phlogopite from a high temperature vapor phase assemblage in alkali olivine basalt. *EOS* **75**, 356.

Traub, I. (1975): Chemische Zusammensetzung natürlicher Pseudobrookite und koexistierender Hämatite. Diploma thesis, unpublished. Mineralogisch-Petrographisches Institut der Universität Heidelberg, 55 pp.

Uher, P., Cerny, P., Chapman, R., Hatar, J. and Miko, O. (1998): Evolution of Nb,Ta-oxide minerals in the Prasiva granitic pegmatites, Slovakia. I. Primary Fe,Ti-rich assemblage. *Canad. Mineral.* **36**, 525–534.

van Kooten, G.K. (1980): Mineralogy, petrology, and geochemistry of an ultrapotassic basaltic suite, Central Sierra Nevada, California, USA. *J. Petrol.* **21**, 651–684.

Venturelli, G., Capedri, S., Barbieri, M., Toscani, L., Salvioli Mariani, E. and Zerbi, M. (1991): The Jumilla lamproite revisited: a petrological oddity. *Eur. J. Mineral.* **3**, 123–145.

von Knorring, O. and Cox, K.G. (1961): Kennedyite, a new mineral of the pseudobrookite series. *Mineral. Mag.* **32**, 676–682.

Wagner, C. and Velde, D. (1985): Mineralogy of two peralkaline, arfvedsonite-bearing minettes. A new occurrence of Zn-rich chromite. *Bull. Minéral.* **108**, 173–187.

Wagner, C. and Velde, D. (1986): The mineralogy of K-richterite-bearing lamproites. *Am. Mineral.* **71**, 17–37.

Received 11 November 2002
Accepted in revised form 20 August 2003
Editorial handling: M. Engi